Pergamon
www.elsevier.nl/locate/asr

Adv. Space Res. Vol. 24, No. 1, pp. 23–33, 1999

Printed in Great Britain
0273-1177/99 $20.00 + 0.00

PII: S0273–1177(99)00418-4

PLASMA WAVES OBSERVED DURING CUSP ENERGETIC PARTICLE EVENTS AND THEIR CORRELATION WITH POLAR AND AKEBONO SATELLITE AND GROUND DATA

J. S. Pickett[1], D. A. Gurnett[1], J. D. Menietti[1], M. J. LeDocq[1], J. D. Scudder[1], L. A. Frank[1], J. B. Sigwarth[1], K. L. Ackerson[1], D. D. Morgan[1], J. R. Franz[2], P. M. Kintner[2], B. T. Tsurutani[3], C. M. Ho[3], J. Chen[4], T. A. Fritz[4], C. T. Russell[5], W. K. Peterson[6], Y. Kasahara[7], I. Kimura[8], S. Watanabe[9], G. G. Arkos[10], G. Rostoker[11], S. Kokubun[12], H. Fukunishi[8], R. F. Pfaff[13], F. S. Mozer[14], S.-Y. Hsieh[15], T. Mukai[15], M. O. Chandler[16]

[1]*The University of Iowa, Department of Physics and Astronomy, Iowa City, IA 52242, USA*
[2]*Cornell University, School of Electrical Engineering, Ithaca, NY 14853 USA*
[3]*Jet Propulsion Laboratory, 4800 Oak Grove Drive, Pasadena, CA 91109 USA*
[4]*Boston University, Center for Space Physics, Boston, MA 02215 USA*
[5]*University of California, L.A., Institute of Geophysics and Planetary Physics, Los Angeles, CA 90095 USA*
[6]*Lockheed Martin Palo Alto Research Laboratory, 3251 Hanover St., Palo Alto, CA 94304 USA*
[7]*Kyoto University, Graduate School of Electronics and Communication, Kyoto 606-01, Japan*
[8]*Osaka Institute of Technology, Osaka, Japan*
[9]*Tohoku University, Department of Geophysics, Aramaki Aoba, Sendai, 980, Japan*
[10]*The University of Calgary, Institute for Space Research, Calgary, Alberta, Canada T2N 1N4*
[11]*The University of Alberta, Department of Physics, Edmonton, Alberta, Canada T6G 2J1*
[12]*Nagoya University, Solar-Terrestrial Environment Laboratory, 3-13 Honohara, Toyokawa, Aichi 442, Japan*
[13]*NASA/Goddard Space Flight Center, Greenbelt, MD 20771*
[14]*University of California, Berkeley, Space Sciences Laboratory, Berkeley, CA 94720 USA*
[15]*Institute of Space and Astronautical Science, Sagamihara, Kanagawa 229, Japan*
[16]*NASA/Marshall Space Flight Center, Huntsville, AL USA*

ABSTRACT

We present Polar plasma wave data during cusp energetic particle (CEP) events at 6-9 R_E. These data suggest the presence of coherent electrostatic structures that are highly localized and that have typical velocities on the order of hundreds to thousands of km/s along the ambient magnetic field. Some of the wave signatures are solitary waves and some are wave packets. The Polar wave instrument also provides evidence that some of the bursts of electromagnetic waves (with frequencies of a few hundred Hz and just below the electron cyclotron frequency around 800 Hz to 1-2 kHz) that are observed are coherent and propagating both up and down the field lines. Electron cyclotron harmonic (ECH) waves are often detected but their duration is usually short (< 1 s). Low Frequency (<1 kHz), broadband, bursty electromagnetic waves are also present. The Polar wave data results are used to obtain a better understanding of the macro/microphysics during a CEP event that takes place on September 11, 1996, by correlating various Polar (~ 7.0 R_E) and Akebono (~ 1.4 R_E) data while both spacecraft are in or near the cusp/cleft region and nearly on the same field line, and magnetometer data from the Canadian Intermagnet and Canopus ground stations, which lie near the base of the magnetic footprint passing through Polar. Solar wind and magnetic field data from the interplanetary medium and magnetosheath are provided by the Geotail and IMP-8 satellites, respectively. Some of the cusp waves may be indicators of the reconnection process taking place through the cusp, the result of mixing of magnetosheath with magnetospheric plasma, and the consequence of an anisotropic electron population in a depressed magnetic field. The low frequency electromagnetic waves are still under study to determine their role, if any, in the heating and acceleration of the MeV He ions during CEP events.

INTRODUCTION

Intense, bursty, broadband electromagnetic waves spanning the range from a few Hz to a few kHz (low frequency magnetic noise) have been observed by the Polar Plasma Wave Instrument (PWI) (Gurnett *et al.*, 1995) in and near the dayside cusp of the Polar orbit. These waves are not seen every orbit, nor are they seen consistently throughout the year. In addition, MeV He^{++} ions have been observed by Polar CAMMICE (Charge and Mass Magnetospheric Ion Composition Experiment) in the cusp, the so-called Cusp Energetic Particle (CEP) events (Chen *et al.*, 1998), that appear to be correlated with a decrease in the total ambient magnetic field as measured by the Polar MFE (Magnetic Field Experiment) instrument (Russell *et al.*, 1995), and with an increase in the low frequency magnetic noise as measured by Polar PWI. To better understand the CEP events, a detailed study of waves observed in the cusp and their role, if any, in the global system was undertaken.

Below we present in detail some of the wave emissions (the microphysical processes) that are seen in the cusp during CEPs with the PWI on the Polar spacecraft. Following this, we review some macrophysical processes occurring during a cusp event that took place around 22:00 UT on September 11, 1996, by presenting various spacecraft and ground data. The present work is not meant to be a rigorous investigation of the macrophysical processes taking place, but rather a top level appraisal of what we believe to be occurring based on the in situ and remote sensing data.

MICROPHYSICAL PROCESSES

Whistler Mode Waves

An example of one type of wave emission observed in the cusp/cleft is seen in Figure 1(A). During this time, the Polar spacecraft was at approximately 8.6 R_E, 80 degrees ILat (Invariant Latitude), 1236 MLT (Magnetic Local Time), and 61 degrees MLat (Magnetic Latitude). This example shows a series of wave packets covering a time period of approximately 160 ms in each of the three orthogonal electric channels (top three panels) and of the three orthogonal magnetic channels (bottom three panels) obtained by the PWI High Frequency Waveform Receiver (HFWR). The time, in decimal seconds, of 01:47:44 UT on September 11, 1996, is plotted on the horizontal axis. The vertical axis contains the magnitude of the electric field, in mV/m, for the first three panels and the magnitude of the magnetic field, in nT, for the last three. The data were calibrated by transforming the uncalibrated waveforms to the frequency domain by means of an FTT, applying the calibrations, and performing an inverse FFT to reproduce the waveform, now calibrated. Antenna lengths (electric only), differential amplifier gains, and dc offsets were taken into account before the initial transformation. This specific example was chosen because the electric channels show the presence of perhaps only one other wave, thus making it clear that the electromagnetic wave is the dominant one at this time. Shown in Figure 1(B) is the index of refraction (cB/E, where c is the speed of light, B is the total measured, fully calibrated, magnetic component, and E is the total measured, fully calibrated, electric component) vs. frequency for the time period shown in Figure 1(A). Here we can see a narrowband peak around 250 Hz at large index of refraction, which is associated with the waveform seen in Figure 1(A).

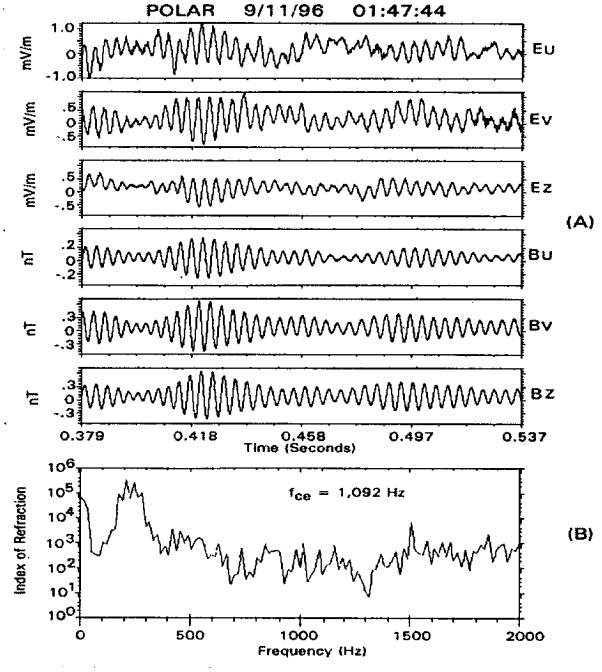

Fig. 1. (A) Waveform and (B) index of refraction of narrowband whistler mode waves at ~200-300 Hz.

Applying an FFT to the waveform shown in Figure 1(A) and employing the analysis algorithm of Means (1972) to the transformed data (LeDocq, 1998), we find that the electromagnetic waves that peak around 200-300 Hz are coherent and right-hand polarized. In addition, they are propagating antiparallel to the magnetic field (within 30

degrees), in this case away from the earth, below the electron cyclotron frequency, f_{ce} (~1.1 kHz), and above the lower hybrid resonance frequency, f_{LHR} (~26 Hz), which means they are most likely whistler mode waves. The index of refraction plotted in Figure 1(B) is consistent with this. The HFWR data confirm that bursts of narrowband whistler mode waves similar to those in Figure 1 are frequently seen in the cusp traveling both up and down the field lines (within about 30 degrees) at frequencies of a few hundred Hz and at frequencies just below f_{ce}. Occasionally, they are seen almost continuously (several seconds).

Although these whistler mode waves have not been reported to have been observed before in the cusp, we believe that they may have been detected but not resolved by the receivers making the measurements. The waves occurring around a few hundred Hz often get masked by the low frequency, broadband, magnetic waves described below. Gurnett and Frank (1978), using a wave receiver on Hawkeye I, observed similar whistler mode waves, lion roars, in the magnetosheath where the broadband magnetic noise is not present.

Electron Cyclotron Harmonic Waves

Another emission frequently observed in the cusp is the narrowband wave that occurs just above the electron cyclotron frequency and its harmonics. An example is shown in Figure 2(A). The data were captured in the time domain and transformed to frequency space by means of a 4096 point FFT spanning 0.13 s. The data are taken from a snapshot obtained on September 11, 1996, at 01:52:01.749 UT while the spacecraft was at about 8.5 R_E, 80 ILat, 1239 MLT and 60 degrees MLat. This figure shows power spectral density vs. frequency up to only 15 kHz, although the filter cutoff is 25 kHz. The fundamental frequency is seen to peak around 1.1 kHz in each of the three electric (top three panels) and three magnetic channels (bottom three panels). The first harmonic is seen in all channels, however weakly in the magnetics. Higher harmonics are observed only in the electric channels and most prominently in the Ev and Ez channels up to about 20 kHz for this example. At this time f_{ce} is about 1.0 kHz (based on Polar MFE data) and f_{pe} about 21.8 kHz (based on Polar Hydra data). Thus, we see that these narrowband waves lie just above f_{ce} and its harmonics. The magnitude of the harmonic peaks falls off with increasing frequency. Although the emissions are observed up to about f_{pe} and f_{UHR}, we cannot draw any conclusions based upon this since the peak intensity is near the noise floor of the receiver at that frequency. The reason for the broadening of the Eu peaks is unknown. Shown in Figure 2(B) is the index of refraction vs. frequency for this example. The sharp depressions seen in the index of refraction occur at the peak frequencies observed in Figure 2(A), and are indicative of electrostatic waves. The observation that the depressions associated with the fundamental and first harmonic are not as deep as the second harmonic is consistent with the influence of the magnetic components.

Further analysis of the magnetic components of the waves occurring at the fundamental frequency was performed using the Means method (1972) (LeDocq, 1998). The results show that the k-vector is nearly perpendicular to the local magnetic field. In addition, when the waveforms are transformed to a magnetic field aligned coordinate system, the electric field emissions are detected primarily in the plane perpendicular to the magnetic field. This information suggests that these narrowband waves could be "Generalized Bernstein Mode" (electromagnetic mode) waves (Stix, 1992), since the fundamental frequency, and sometimes the first harmonics, are resolved in the magnetic channels and because the bands lie just above f_{ce} and its harmonics. The electromagnetic modes are merely an indication that the electrostatic criteria ($k_\perp$ sufficiently large) are not fully satisfied, but nearly so as to give an index of refraction that would suggest the

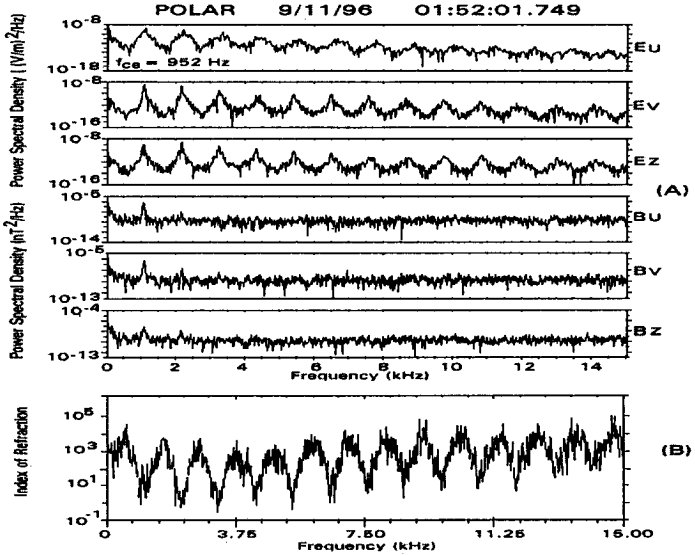

Fig. 2. (A) Power Spectral Density and (B) index of refraction of electron cyclotron harmonic waves.

waves are electrostatic. The narrowband waves shown in Figure 2(A) are typical of those encountered in the cusp regions during CEP events, although the magnetic components are not always present, perhaps because they are weak and fall below the noise floor of the receiver. The location of the harmonic bands in frequency space is a function of density, temperature and field strength.

Electrostatic electron cyclotron (Bernstein mode) waves occurring just above f_{ce}, sometimes with a weak harmonic, have been reported in the cusp by Gurnett and Frank (1978). Electrostatic electron cyclotron waves in the central part of the cusp have also been reported by Pottelette *et al.*, 1990. This may be the first time these waves have been observed in the cusp with the electric field component having so many harmonics and with a magnetic field component with at least one harmonic. Shaw and Gurnett (1975) observed a weak magnetic component associated with electrostatic noise bands in the outer magnetosphere. However, the magnetic component was detected in only 8 cases in their survey of the IMP-6 wave data. Matsumoto and Usui (1997) reported the observation of ECH waves at the dayside equatorial magnetopause region using Geotail data. These waves appear very similar to the ones reported here (narrowband, multiple harmonics with a magnetic component) and were termed "totem pole" emissions.

Coherent Electric Field Structures

A type of waveform typically seen by Polar PWI in the cusp is the bipolar pulse as shown in the PWI interferometry data of Figure 3, top two panels. These data were taken on September 22, 1996, during a CEP event and comprise a small portion of the 1.2 s. snapshot taken at 01:14:42.8210 when the spacecraft was at 8.5 R_E, 80 degrees ILat, 1155 MLT, and 60 degrees MLat. Elapsed time since the start of the snapshot is plotted on the horizontal axis. The baseline of the interferometer is 50 m which is the distance between each of the Ev+ and Ev- antenna spheres and the spacecraft body. During the time interval shown in Figure 3, the interferometer baseline (Ev+ and Ev- antennas) was nearly parallel with the magnetic field (within 20 degrees). This allows us to calculate the velocity and parallel widths with less error. Using the cross correlation technique employed in Franz *et al.* (1998) and LaBelle and Kintner (1989), the delay time of -196 microseconds from when Ev+ detects the wave in relation to Ev- (bottom panel of Figure 3), and the fact that Ev- sees the wave first in this particular configuration with respect to **B**, tells us that the wave is a positive structure traveling down the field (toward the earth) with a velocity of about 200 km/s and has a parallel width on the order of 60 m. This is a one dimensional picture of the wave since only the electric v-antenna is in the interferometry mode (see Franz *et al.*, 1998). An FFT of these pulses is what produces a typical broadband spectrum in the electric field with no discernible magnetic field component, the so-called Broadband Electrostatic Noise (BEN). Gurnett and Frank (1978) observed BEN in the cusp using the Hawkeye I data but did not associate it with the bipolar, solitary type structures recently observed in the cusp and various other regions of the magnetosphere (Franz *et al.*, 1998, Tsurutani *et al.*, 1998, Pottelette and Treumann, 1998, Mozer *et al.*, 1997, Matsumoto *et al.*, 1994, Ergun *et al.*, 1998).

Low Frequency Waves

Intense, low frequency, broadband (ULF-VLF) waves covering the entire range of the PWI 6 channel Low Frequency Waveform Receiver (LFWR) of 0.1 to 25 Hz and from the lowest frequency measured (5.6 Hz) to several hundred Hz of the Multi-Channel Analyzer (MCA) are almost always seen in the cusp regions where the magnetic field is depressed and noisy. These waves are electromagnetic with peak intensity occurring at the lowest frequencies measured by each of the receivers and with intensity decreasing rapidly with increasing frequency. A spectrogram of data taken by the MCA (1.3 s per spectrum) connected to the BU magnetic search coil on September 11, 1996, from 21:30 to 22:30 UT is shown in Figure 4 (see the bottom of Figure 6 for location and magnetic information). This spectrogram clearly shows the burstiness and broadbandedness of these low frequency waves from 5.6 Hz up to about 200 Hz throughout the period of 21:45 through 22:15 UT. Also seen in this figure are the narrowband bursts of whistler mode waves just below f_{ce} (white line trace)

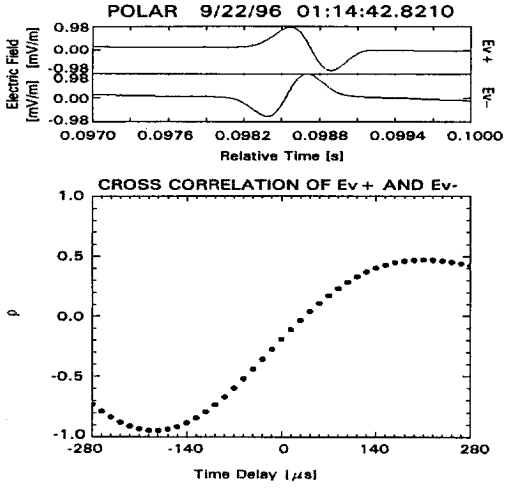

Fig. 3. Bipolar waveforms and time delay interferometry data of coherent electric field structures.

and around 200-300 Hz, which are obscured by the broadband waves, as described above. The broadband low frequency waves are the ones that Chen *et al.* (1998) reported as usually being correlated with the CEP events.

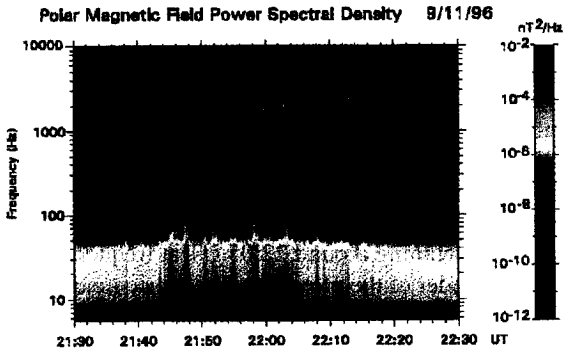

Fig. 4. Wave magnetic field spectrogram showing bursty, broadband low frequency waves.

We have not yet identified the mode of the waves seen in Figure 4 since waveforms are not available from the MCA. However, LFWR data covering the low frequency range of the MCA (<25 Hz) show that the waveforms are not sinusoidal and sometimes appear pluse-like. Thus these emissions may be an indication of structures associated with Alfven, ion cyclotron or lower hybrid waves, which occur in this frequency range. Pfaff *et al.* (1998) have identified similar ULF-VLF (< few Hz) waves in the cusp using measurements from the Polar electric and magnetic field experiments, and have tentatively identified them as Alfven waves. D'Angelo *et al.* (1974) reported observations from Ogo 5 in which ULF magnetic fluctuations were detected at the polar cusp boundaries and probably due to the Kevin-Helmholtz instability. Gurnett and Frank (1978) reported the presence of a band of ULF-ELF magnetic noise extending from a few Hertz to several hundred Hertz almost every cusp pass using Hawkeye I data. They stated that this noise can be used as a reliable indicator of the polar cusp region. They speculated that since this noise cuts off just below f_{ce} that it must consist of whistler mode electromagnetic waves. Similar waves detected along auroral field lines (Gurnett *et al.*, 1984) were tentatively identified as Alfven waves.

MACROPHYSICAL PROCESSES

We now examine a specific dynamic cusp event on September 11, 1996, around 22:00 UT. Figure 5 provides a schematic of the locations of the various spacecraft with respect to the magnetopause and bow shock of Earth.

Magnetosphere

A one hour plot from 21:30 to 22:30 UT on September 11, 1996, of data from various science instruments on POLAR is presented in Figure 6. From top to bottom the panels are: 1) high time resolution (54 Hz) total magnetic field data from MFE, in nT; 2) 0.52-1.15 MeV He^{++} flux from CAMMICE, in $(cm^2\text{-sr-s})^{-1}$; 3) and 4) flux of mass resolved H^+ and He^{++} ions, respectively, from over 98% of the full solid angle over the energy range 15 eV/e to 33 keV/e in logarithmically-spaced steps denoted by energy steps 0-27 on the left side from TIMAS, Toroidal Imaging Mass-Angle Spectrograph (Shelley *et al.* 1995), in units of $(cm^2\text{-sr-s-keV/e})^{-1}$; 5) total electron flux over the full solid angle using 12 discrete sensor modules in the energy range 12 eV to 18 keV from Hydra (Scudder *et al.*, 1995), in units of $(cm^2\ s\ sr\ keV)^{-1}$; 6) power spectral density of one of the electric components (Eu) in the spin plane for waves in the frequency range 5.6 Hz to 311 kHz from PWI, in $(V/m)^2/Hz$.

The TIMAS ion and Hydra electron data show that Polar was in the cusp until about 22:28 UT based on the presence of solar wind origin ions of several keV/e and several tens of eV electrons, respectively. Note that the color white in the TIMAS data (panels 3 and 4), indicates regions of uncorrected non-linear response and intensities

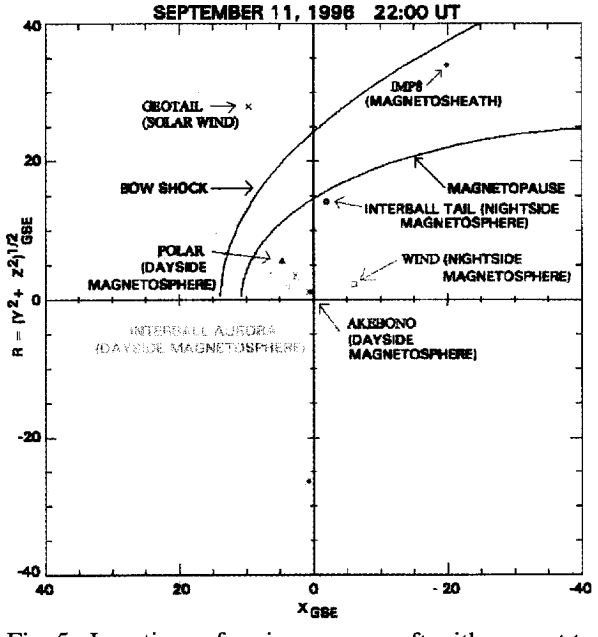

Fig. 5. Locations of various spacecraft with respect to the bow shock and magnetopause.

greater than that of red. Relative TIMAS fluxes in other regions are accurately indicated by the color bar on the right. Polar was also in a diamagnetic cavity from 21:58 to 22:05 UT during which time the magnetic field was depressed, the wave electric field, BEN, was decreased in intensity and frequency, and the ions and electrons appeared more intense and covered a broader energy range. The flux of MeV ions (panel 2) also rapidly increased. The reduction of the BEN and magnetic field is more representative of the cusp interior or proper. The sudden change at ~21:58 UT may thus indicate that the cusp has expanded (or that its boundary has shifted), allowing Polar to observe the more intense interior cusp ions and electrons in the absence of the strong electric field waves typically seen on the boundaries. Also, we note the presence of auroral kilometric radiation (AKR) throughout the hour which becomes very intense beginning around 22:05 UT at frequencies above about 100 kHz and continuing quite strong through most of the remainder of the plot. The dc electric field (not shown) as measured by EFI, Electric Field Instrument (Harvey *et al.*, 1995) during the hour in both the spin plane and perpendicular to it was near zero and noisy (most perturbations $\bar{\times}\lesssim 5$ mV/m p-p). To complete the picture at Polar's location, images taken with the VIS Earth Camera (Frank *et al.*, 1995) at 130.4 nm show a substorm onset at about 21:57:18 UT (previously the aurora had been quiet) near dusk at approximately 18 MLT. At ~ 22:05:15 UT, the aurora is in expansion as the oval brightens poleward.

A magnetic conjunction of Polar and Akebono (1.4 R_E) was predicted to have occurred at about 21:53 to 21:54 UT. Figure 7 shows particle and wave data for the period 21:48:54 to 2202:14 UT on September 11, 1996. The wave data shown in the top two panels are from the MCA receiver, which is one of the subsystems of the VLF instrument onboard Akebono (Kimura *et al.*, 1990). It provides one component of the electric field (top panel) and one of the magnetic field (bottom panel) at 16 frequency points with color indicating the magnitude of the electric and magnetic field, respectively. Weak, bursty electric field waves (BEN) are observed from the lowest frequency measured by the

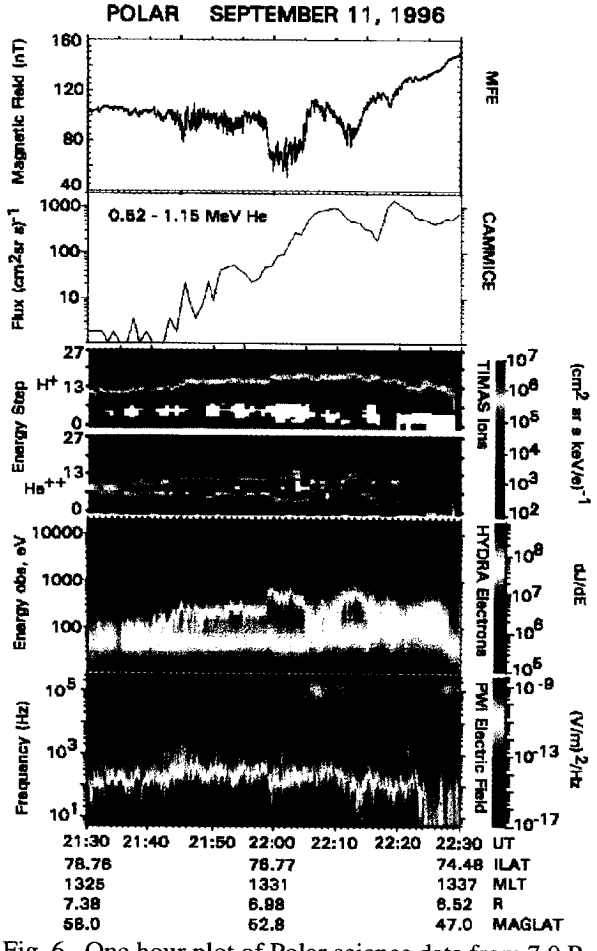

Fig. 6. One hour plot of Polar science data from 7.0 R_E during a cusp crossing that contains a diamagnetic cavity.

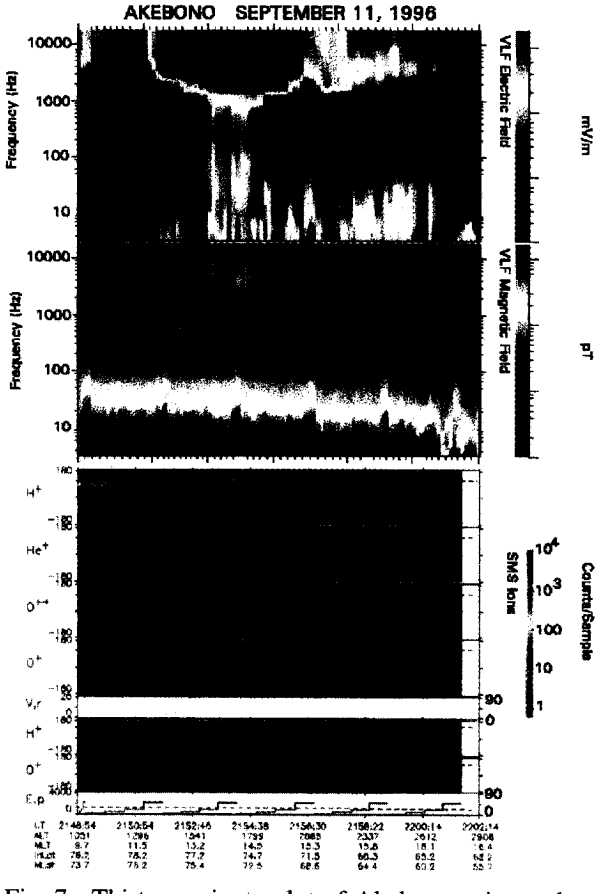

Fig. 7. Thirteen minute plot of Akebono science data from 1.4 R_E for the cusp event of Fig. 6.

detector, 3.16 Hz, to a hundred Hz throughout much of the interval, but a definite end to these waves occurs about 22:01 UT. Intense electromagnetic emissions observed above 1 kHz in both the electric and magnetic channels up to about 21:58 UT are probably whistler mode hiss. Intense magnetic field waves are observed throughout the entire interval at frequencies below about 100 Hz. The periodically-spaced spikes seen in the magnetic data are due to interference from another instrument. The bottom panels of Figure 7 show ion data from the Akebono Suprathermal Ion Mass Spectrometer, SMS, (Whalen *et al.*, 1990). The first four panels are the thermal energy (< 25 eV) channels for H^+, He^+, O^{++} and O^+ ions and the sixth and seventh panels are the suprathermal channels (> 25 eV) for H^+ and O^+. The vertical axis for these panels corresponds to spin phase, from -180 to +180 degrees, where 0 degrees is defined as the direction at which ions with smallest pitch angles are observed. The dashed blue line at about 100 degrees is the phase angle corresponding to the "ram" direction. The SMS panels show primarily thermal H^+ prior to about 21:59 UT. These ions are observed to be roughly oriented upward and in the ram direction. They are believed to be co-rotating, i.e., approximately stationary in a frame chosen to be co-rotational with the earth. The obvious change observed in all ion channels at 21:59 UT is most likely due to energetic ions from the radiation belts moving along closed field lines (consistent with the wave data) at lower latitudes, although another possible reason is noise due to neutrals because of the low altitude. Because the sudden change occurs almost at the same time as when Polar observes the diamagnetic cavity, we believe that Akebono most likely encountered closed field lines earlier than expected due to movement of the field lines. We should note that the micro-channel plate (MCP) detector portion of the SMS is well past its design lifetime, and as such has shown a steady decrease in sensitivity, reflected in lower overall ion counts.

Several other spacecraft located in Earth's magnetosphere detected significant increases in particle energy and flux at approximately 22:00 UT on September 11, 1996. Interball Tail, for example, was located at the nightside magnetopause (see Figure 5) and detected unusually strong boundary layer/cleft signatures from 17:00 to 21:00 UT and crossed the magnetopause/boundary layer around 22:00 UT, the time when Polar and Akebono detected significant disturbances (S. Savin, Personal Communication, 1998). The state of the magnetosphere as determined by the Kp index was 4+ at this time. In addition, the Dst index was -39 nT. Both of these indices indicate that the magnetosphere was moderately disturbed, which is consistent with the auroral images.

Interplanetary and Magnetosheath

The interplanetary magnetic field as measured by the Geotail MGF instrument (Kokubun *et al.*, 1994) is presented in Figure 8. According to Figure 5, Geotail was just outside the bow shock, about 27 R_E dawnward of the Earth-Sun line. The GSM B_X and B_Y components are seen to be negative and highly positive, respectively, throughout the entire interval from 21:30 to 22:30 UT. However, the B_Z component is primarily slightly negative until about 22:12 UT, positive for about 10 minutes and then negative again. IMP-8 in the magnetosheath observed the same types of fields with the exception that B_Z was positive until 22:12 UT (allowing for a time lag estimated to be about 11 minutes between the two spacecraft). The reason for the difference in the sign of Bz as measured by each spacecraft up to 22:12 UT has not been determined but most likely is related to the high degree of fluctuation observed in the IMF during that time (Figure 8) and reconnection at earth. Using Geotail MGF data, we find that the cone angle, the angle between IMF and the earth-sun line, throughout the entire hour is ≥ 50 degrees. In addition, the dipole tilt angle (angle of the north magnetic pole to the GSM Z-axis, positive when the north magnetic pole is titled toward the sun) for the entire interval varies from 7.4 degrees at 21:30 to 4.7 degrees at 22:30 UT. This means that the dayside cusp is somewhat tilted toward the sun, which would allow for easier access of the solar wind to the cusp. The solar wind as measured by the Geotail CPI instrument (Frank *et al.*, 1994) was shown to be quite steady with a density of about 5-6 cm^{-3}, an ion temperature of 3 x 10^5 Kelvin, and a speed of about 570 km/s directed along the Earth-Sun line. This is slightly higher than average.

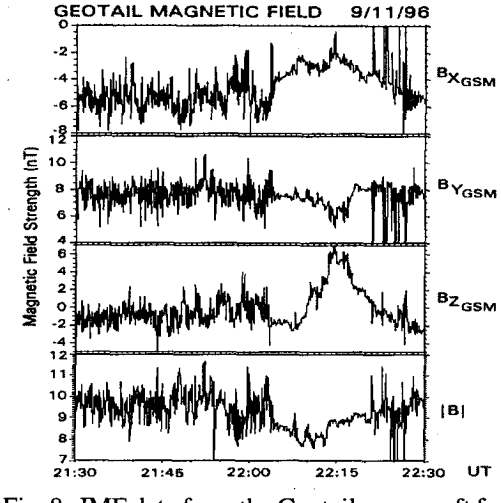

Fig. 8. IMF data from the Geotail spacecraft for the cusp event of Fig. 6.

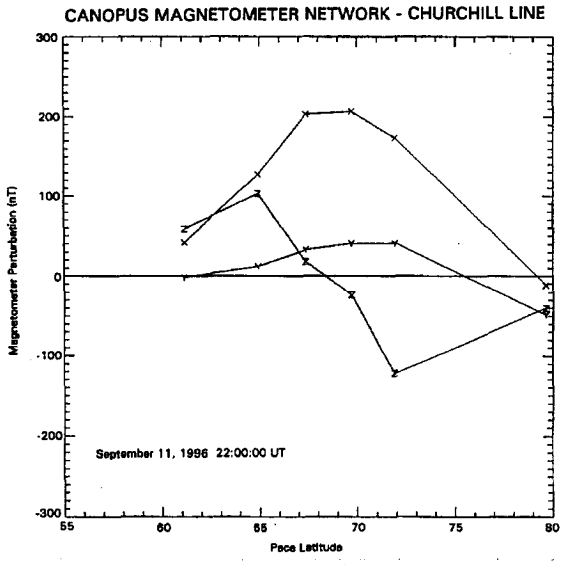

Fig. 9. Latitude profiles from the Canopus magnetometer network in Canada for the cusp event of Fig. 6.

Ground Magnetometer Measurements

The base of the magnetic footprint of the POLAR spacecraft was projected to have been over the Intermagnet geomagnetic observatory network ground station of Cambridge Bay, Canada (69.1 degrees geographic latitude [under the cleft region], 255.0 degrees geographic longitude) at about 22:00 UT. Data from this station show that starting at about 20:00 UT, there is a magnetic signature of eastward ionospheric current across the noon sector, the so-called DPY current (Belehaki and Rostoker, 1996). A latitude profile from the Canopus ground magnetometer network (Rostoker et al, 1995) Churchill line (one time zone east of the Cambridge Bay meridian) is shown in Figure 9. The plot shows magnetometer perturbation vs. Pace Latitude (≈ invariant latitude) for each of the X, Y and Z components at five sites at 22:00:00 UT on September 11, 1996. Here we see that the eastward DPY current is centered at ~ 69 degrees Pace latitude, with an equatorward edge around 65 degrees North and a poleward edge north of 73 degrees North by about 1-2 degrees. Canopus data were also filtered in the pi 2/pc 5 frequency band for this same date to see what, if any, impulsive responses were observed around 22:00 UT. Although not shown here, there was a significant burst of pulsation activity initiated between 22:00 and 22:05 UT as detected by many of the Canopus stations. In fact, there was quite significant pulsation activity throughout the interval 2000-2400 UT. However, the only time activity is significantly enhanced at high (cleft type) latitudes is around the 22:00 to 22:05 UT time period. This suggests some dynamic behavior in the cleft region at this time, and possibly mixed spatial and temporal effects.

DISCUSSION AND CONCLUSIONS

The narrowband whistler mode waves detected by PWI at frequencies < 500 Hz and just below f_{ce} may be a result of an elec tron cyclotron instability that is caused by an anisotropic electron population of shocked solar wind origin. Figure 10 shows a plot, by panels, of total anisotropy ($P_{\parallel}/P_{\perp}$, where $P_{\parallel}$ and $P_{\perp}$ are the parallel and perpendicular particle pressures, respectively), total parallel pressure (black trace) and total perpendicular pressure (red trace), and magnetic pressure (green) and total particle pressure (black). These pressures were derived from Polar Hydra and MFE data. This plot shows that a total particle anisotropy does exist during the hour in which the narrowband whistler mode waves are observed. Most of the whistler mode waves seen in Figure 4 are observed during the periods of time when $P_{\parallel}/P_{\perp}<1$ which is consistent with an electron cyclotron instability. Similar whistler mode waves are often observed in the magnetosheath (Smith and Tsurutani, 1976; Rodriguez, 1985; Zhang *et al.*, 1998a) and are referred to as "lion roars" and in the upstream of the bow shock (e.g., Zhang et al., 1998b). We do not rule out the possibility that these waves are produced by some other instability, such as the firehose instability, since a statistical analysis has not yet been performed to determine the probable instability in all cases. We also do not rule out the possibility that the instability responsible for the whistler mode

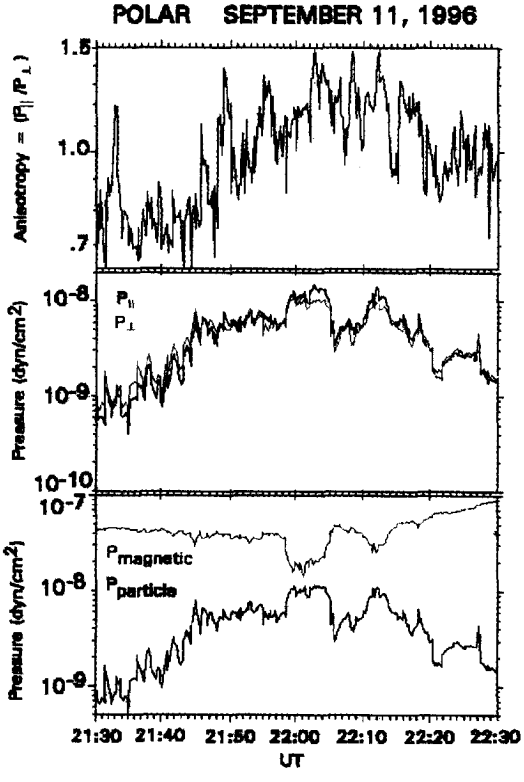

Fig. 10. Anisotropy and pressure data for the cusp event of Fig. 6.

waves <500 Hz is the same one responsible for those just below f_{ce}.

The presence of ECH waves in the cusp is an indication that the plasma conditions are changing on relatively short time scales. In these depressed magnetic field regions with a persistent $\nabla\mathbf{B}$ or large field curvature, variations of the electron pressure anisotropy and gyrotropy are often observed (Scudder *et al.*, 1998), which could generate ECH waves. Another possibility is that the instability that gives rise to electron Bernstein mode waves might be very sensitive to an admixture of cold plasma with the hot anisotropic electron distribution (Ashour-Abdalla *et al.*, 1979) as might be observed in the cusp. Matsumoto et al. (1997) speculated that similar ECH waves at the dayside magnetopause were an electrostatic X mode and that the weak magnetic component was due to the spatial rotation of the wave electric field component in the plane perpendicular to Bo.

As we have seen, bipolar pulses in the PWI data are associated with coherent electric field structures that move both up and down the geomagnetic field, sometimes simultaneously, at velocities the order of 1000 km/s (the velocity of a 6 eV electron) (Franz *et al.*, 1998). These waves are the ones that contribute to the spectral features of broadband electrostatic noise that has often been observed in many regions of the magnetosphere. In the low altitude cleft (1-2 R_E) these electrostatic bursts, measured by the wave instrument on Viking have been correlated with 0.1 to 1 keV electron beams and with small-scale field-aligned currents, and is always associated with low-frequency (~1 Hz) electric field fluctuations (Pottelette *et al.*, 1990). Perpendicular acceleration of ambient plasma ions occurs in connection with the bursts. Pottelette and Treumann (1998) state that the BEN emissions appear to be the "messengers" of the reconnection process occurring along the magnetic field lines which are connected to the reconnection sites since BEN is always related to field-aligned electron fluxes.

The ULF-VLF waves observed by Polar PWI may be an indication of structures associated with Alfven, ion cyclotron or lower hybrid waves. Whether these waves would be sufficient to accelerate ions to the energies seen during CEP events is still under investigation. We note, however, that Chang *et al.* (1998) have suggested that the MeV He^{++} ions reported by Chen *et al.* (1998) in the cusp can be explained by convection and well-known processes occurring at the Earth's bow shock. Similar ULF-VLF waves have associated with transverse acceleration of ions from thermal energies to 32 keV on Polar at altitudes greater than 20,000 km (Huddleston et al., 1998).

Auroral kilometric radiation often seen in the cusp by Polar PWI can usually be associated with auroral substorms. The onset of intense AKR seen around 22:05 UT is consistent with the substorm expansion onset as determined from the VIS images. Since the AKR source region is at a much lower altitude, the AKR observed by PWI in the northern cusp has obviously propagated from an area far beneath the spacecraft. The ground magnetometer data also provide evidence that prior to the substorm expansion, a DPY ionospheric current was flowing across noon. Based on Belehaki and Rostoker (1996), the DPY current is an extension of one of the auroral electrojets across noon, in this case eastward based on a positive IMF BY.

ACKNOWLEDGMENTS

Funding for this study has come from several sources which we would like to acknowledge: NASA/GSFC under several contracts and grants, primarily NAS5-30371, Institute of Space and Astronautical Science Institute, Canadian Space Agency, and the Geological Survey of Canada. We thank R. P. Lepping for the use of the IMP-8 magnetic field data. JSP thanks Julie Dowell and Larry Granroth at Iowa for providing the numerous software routines for PWI data retrieval and the engineering staff at Iowa for providing the extremely complicated PWI calibrations. JSP would also like to thank the PAPCO software development team and the entire ISTP project team for providing the necessary tools, such as PAPCO, SSCWeb and CDAWeb, for performing an ISTP study of this type.

REFERENCES

Ashour-Abdalla, M., C. F. Kennel, and W. Livesey, A Parametric Study of Electron Multiharmonic Instabilities in the Magnetosphere, *J. Geophys. Res.*, **84**, 6540 (1979).

Belehaki, A., and G. Rostoker, Relationship Between the Dayside Auroral Electrojets and the DPY Current, *J. Res.*, **101**, 2397 (1996).

Chang, S.-W., J. D. Scudder, S. A. Fuselier, J. F. Fennell, K. J. Trattner, *et al.*, Cusp Energetic Ions: A Bow Shock Source, *Geophys. Res. Lett.*, submitted, 1998.

Chen, J., T. A. Fritz, R. B. Sheldon, H. E. Spence, W. N. Spjeldvik, *et al.*, Cusp Energetic Particle Events: Implications for a Major Acceleration Region of the Magnetosphere, *J. Geophys. Res.* **103**, 69 (1998).

D'Angelo, N., A. Bahnsen, and H. Rosenbauer, Wave and Particle Measurements at the Polar Cusp, *J. Geophys. Res.*, **79**, 3129 (1974).

Ergun, R. E., C. W. Carlson, J. P. McFadden, F. S. Mozer, G. T. Delory, *et al.*, FAST Satellite Observations of Large-amplitude Solitary Structures, *Geophys. Res. Lett.*, **25**, 2041 (1998).

Frank, L. A., K. L. Ackerson, W. R. Paterson, J. A. Lee, M. R. English, *et al.*, The Comprehensive Plasma Instrumentation (CPI) for the Geotail Spacecraft, *J Geomag. And Geoelec.*, **46**, 23 (1994).

Frank, L. A., J. B. Sigwarth, J. D. Craven, J. P. Cravens, J. S. Dolan, *et al.*, The Visible Imaging System (VIS) for the Polar Spacecraft, *Space Science Rev.*, **71**, 297 (1995).

Franz, J. R., P. M. Kintner, and J. S. Pickett, POLAR Observations of Coherent Electric Field Structures, *Geophys. Res. Lett.*, **25**, 1277 (1998).

Gurnett, D. A., and L. A. Frank, Plasma Waves in the Polar Cusp: Observations from Hawkeye I, *J. Geophys. Res.* **83**, 1447 (1978).

Gurnett, D. A., R. L. Huff, J. D. Menietti, J. L. Burch, J. D. Winningham, *et al.*, Correlated Low-Frequency Electric and Magnetic Noise Along the Auroral Field Lines, *J. Geophys. Res.*, **89**, 8971 (1984).

Gurnett, D. A., A. M. Persoon, R. F. Randall, D. L. Odem, S. L. Remington, *et al.*, The Polar Plasma Wave Instrument, *Space Science Rev.*, **71**, 597 (1995).

Harvey, P., F. S. Mozer, D. Pankow, J. Wygant, N. C. Maynard, *et al.*, The Electric Field Instrument on the POLAR satellite, *Space Science Rev.*, **71**, 483 (1995).

Huddleston, M. M., C. J. Pollock, J. S. Pickett, J. L. Burch, D. L. Dempsey, *et al.*, Transversely Accelerated Auroral Ions Observed at High Altitudes by Instruments on the Polar Spacecraft, *EOS Transactions*, **79**, F769 (1998).

Kimura, I., K. Hashimoto, I. Nagano, T. Okada, M. Yamamoto, *et al.*, VLF Observations by the Akebono (EXOS-D) Satellite, *J. Geomag. Geoelectr.*, **42**, 459 (1990).

Kokubun, S., T. Yamamoto, M. H. Acuna, K. Hayashi, K. Shiokawa *et al.*, The GEOTAIL Magnetic Field Experiment, *J. Geomag. Geoelectr.*, **46**, 7 (1994).

LaBelle, J., and P. M. Kintner, The Measurement of Wavelength in Space Plasmas, *Rev. Geophys.*, **27**, 495 (1989).

LeDocq, M., *The Wave Normal and Poynting Flux of Magnetospheric Plasma Waves*, Ph.D. Thesis, The University of Iowa, Iowa City, IA (1998).

Matsumoto, H., H. Kojima, T. Miyatake, Y. Omura, M. Okada, *et al.*, Electrostatic Solitary Waves (ESW) in the Magnetotail: BEN Wave Forms Observed by GEOTAIL, *Geophys. Res. Lett.*, **21**, 2915 (1994).

Matsumoto, H., and H. Usui, Intense Bursts of Electron Cyclotron Harmonic Waves Near the Dayside Magnetopause Observed by Geotail, *Geophys. Res. Lett.*, **24**, 49 (1997).

Means, J. D., Use of the Three-Dimensional Covariance Matrix in Analyzing the Polarization Properties of Plane Waves, *J. Geophys. Res.*, **77**, 5551 (1972).

Mozer, F. S., R. Ergun, M. Temerin, C. Cattell, J. Dombeck, *et al.*, New Features of Time Domain Electric-Field Structures in the Auroral Acceleration Region, *Phys. Rev. Lett.*, **79**, 1281 (1997).

Pfaff, R., S.-Y. Hsieh, J. Clemmons, J. Scudder, C. Kletzing, *et al.*, ULF/VLF Electric Field Signatures in the High Altitude Cusp (Abstract),*EOS Trans. AGU*, **79**, S312 (1998).

Pottelette, R., M. Malingre, N. Dubouloz, B. Aparicio, R. Lundin, *et al.*, High-Frequency Waves in the Cusp/Cleft Regions, *J. Geophys. Res.*, **95**, 5957 (1990).

Pottelette, R., and R. A. Treumann, Impulsive Broadband Electrostatic noise in the Cleft: A Signature of Dayside Reconnection, *J. Geophys. Res.*, **103**, 9299 (1998).

Rodriguez, P., Long Duration Lion Roars Associated with Quasi-Perpendicular Bow Shocks,. *J. Geophys. Res.*, **90**, 241, 1985.

Rostoker, G., J. C. Samson, F. Creutzberg, T. J. Hughes, D. R. McDiarmid, *et al.*, Canopus - A Ground-Based Instrument Array for Remote Sensing the High Latitude Ionosphere during the ISTP/GGS Program, *Space Science Rev.*, **71**, 761 (1995).

Russell, C. T., R. C. Snare, J. D. Means, D. Pierce, D. Dearborn, *et al.*, The GGS/Polar Magnetic Fields Investigation, *Space Science Rev.*, **71**, 563 (1995).

Scudder, J., F. Hunsacker, G. Miller, J. Lobell, T. Zawistowski, *et al.*, HYDRA - A 3-Dimensional Electron and Ion Hot Plasma Instrument for the Polar Spacecraft of the GGS Mission, *Space Science Rev.*, **71**, 459 (1995).

Scudder, J. D., P. Puhl-Quinn, J. C. Dorelli, H. J. Cai, S.-W, Chang, *et al.*, Reconnection Layer Geometry, Topology, Flow Characteristics and Penetration of the Diffusion Region for Northward IMF Poleward of the Cusp (abstract), *EOS Trans. AGU*, **79**, S329 (1998).

Shaw, R.R., and D. A. Gurnett, Electrostatic Noise Bands Associated with the Electron Gyrofrequency and Plasma Frequency in the Outer Magnetosphere, *J. Geophys. Res.*, **80**, 4259 (1975).

Shelley, E. G., A. G. Ghielmetti, H. Balsiger, R. K. Black, J. A. Bowles, *et al.*, The Toroidal Imaging Mass-Angle Spectrograph (TIMAS) for the Polar Mission, *Space Science Rev.*, **71**, 497 (1995).

Smith, E. J., and B. T. Tsurutani, Magnetosheath Lion Roars, *J. Geophys. Res.*, **81**, 2261 (1976).

Stix, T. H., *Waves in Plasmas*, American Institute of Physics, New York, NY (1992).

Tsurutani, B. T., C. M. Ho, G. S. Lakhina, B. Buti, J. K. Arballo, et al., Plasma Waves in the Dayside Polar Cap Boundary Layer: Bipolar and Monopolar Electric Pulses and Whistler Mode Waves, *Geophys. Res. Lett.*, **25**, 4117 (1998).

Whalen, B. A., J. A. Burrows, A. W. Yau, E. E. Budzinski, A. M. Pilon, *et al.*, The Suprathermal Ion Mass Spectrometer (SMS) Onboard the Akebono (EXOS-D) Satellite, *J. Geomag. Geoelectr.*, **42**, 511 (1990).

Zhang, Y., H. Matsumoto, and H. Kojima, Lion Roars in the Magnetosheath: The Geotail Observations, *J. Geophy. Res.*, **103**, 4615 (1998a).

Zhang, Y., H. Matsumoto, and H. Kojima, Bursts of Whistler Mode Waves in the Upstream of the Bow Shock: Geotail Observations, *J. Geophys. Res.*, **103**, 20529 (1998b).